CONF-860522--8

RESIDUAL EFFECTS OF CHROMIUM GETTERING ON THE OUTGASSING BEHAVIOR OF A STAINLESS STEEL VACUUM VESSEL*

J. E. Simpkins
Oak Ridge National Laboratory, Oak Ridge, TN 37831

W R. Blanchard, H. F. Dylla, and P. H. LaMarche
Princeton Plasma Physics Laboratory, Princeton, NY 08544

CONF-860522--8

DE86 011509

Long-lasting beneficial effects on plasmas after chromium gettering have been observed in ISX and TFTR. These benefits include a reduction in radiated power, lower Z_{eff}, and the capability to operate at higher densities. This paper reports laboratory experiments performed to further investigate the underlying mechanism for this enhanced plasma performance. A stainless steel vacuum vessel and a chromium sublimation source were assembled to simulate the arrangement in TFTR. A controlled air leak was introduced, and the residual gases were monitored by a quadruple mass spectrometer before, during, and after the deposition of a chromium film that covered 50% of the vacuum wall. The pumping speed of the film and the amount of gas sorbed as functions of time are shown. Rate-of-rise measurements were made before deposition and after saturation of the film with oxygen. The results indicate that the residual effects of the chromium film on the vacuum are due to reduced outgassing of the stainless steel surface.

* Research sponsored by the Office of Fusion Energy, U.S. Department of Energy, under contract DE-AC05-84OR21400 with Martin Marietta Energy Systems, Incorporated.

* This work supported by U.S. Department of Energy, under Contract No. DE-AC02-CH03073.

DISCLAIMER

1. INTRODUCTION

Laboratory experiments that compared chromium and titanium gettering showed that with chromium, unlike titanium, there is no appreciable diffusion of hydrogen isotopes into the film. It was concluded from these experiments that chromium gettering on tokamaks is more desirable than titanium gettering, since chromium should provide higher hydrogen recycling, minimize tritium inventories, and avoid hydrogen embrittlement [1].

Large-scale sublimation sources, consisting of hollow elongated chromium spheres with internal resistance heaters, were developed for use on tokamaks [2]. These sources have been used to getter both the Impurity Study Experiment (ISX) [3] and the Tokamak Fusion Test Reactor (TFTR) [4]. In both cases, significant effects on plasma performance were observed, including lower Z_{eff} and radiated power losses and an increase in the density limit. In TFTR these effects were observed for a period of weeks after a single chromium deposition.

This paper reports the results of laboratory experiments made to examine the gettering characteristics of chromium films under conditions simulating those in TFTR.

2. EXPERIMENTAL PROCEDURE

A cylindrical stainless steel, bakeable vacuum system housed the experiments and is shown in Fig. 1. The main pump (TMP-1), a 350-L/s turbomolecular pump, was used to pump down the system but was always isolated during the experiments. The chromium sublimation source, described in Section 1, was mounted in the geometric center of the vacuum chamber together with a shield, so that the chromium deposition covered approximately half the interior wall. A small turbomolecular pump (TMP-2) with an effective pumping speed of 7.2 L/s was used as an auxiliary pump to handle gases not pumped by the chromium getter film and to provide a satisfactory equilibrium pressure after film saturation by a gas species. A quadrupole mass spectrometer (RGA) was mounted 180° from the auxiliary pump and behind the source shield. During experiments, the RGA was isolated from TMP-3 and opened to the main chamber. A total pressure gauge was mounted on the vacuum vessel, and a second gauge was mounted on the RGA. The vacuum gauges and the RGA were calibrated by a procedure developed for use on TFTR [5]. A manually operated precision leak valve [6] was preset to introduce the desired flow of either

nitrogen or air, depending upon the experiment. The flow rate was determined by rate-of-rise measurements. The pumping speed of each pump was determined by measuring the equilibrium pressure of the vessel with a known gas flow rate.

The goal of these experiments was to examine the vacuum characteristics of this system before, during, and after chromium gettering in order to explain the long-term effects of the getter film in TFTR. Air was selected as the leak gas in order to simulate the conditions in TFTR, although this choice made the analysis more difficult. Rate-of-rise measurements of the total pressure and the individual gas components were made before gettering to serve as a baseline for comparisons with similar measurements made during and after film saturation. Partial pressure scans and total pressure measurements (using IG2) were made as functions of time starting just before the introduction of the leak gas, throughout film deposition, and until film saturation.

With the partial pressure data, the pumping speed of a gas species $S_{\mathrm{get}_{(i)}}$ (L/s) was computed:

$$S_{\mathrm{get}_{(i)}} = \frac{Q_{\mathrm{leak}_{(i)}}}{P_{(i)}} - S_{\mathrm{aux}_{(i)}} \ , \tag{1}$$

where $Q_{\mathrm{leak}_{(i)}}$ is the leak rate (torr·L/s), $P_{(i)}$ is pressure (torr), and $S_{\mathrm{aux}_{(i)}}$ is the auxiliary pumping speed for gas species (i). The surface coverage θ_t, the ratio of the total number of absorbed particles to the absorbing surface, was also computed as

$$\theta_t = 3.5 \times 10^{19} \times \frac{Q_{\mathrm{leak}_{(i)}} t - S_{\mathrm{aux}_{(i)}} \int_0^t P_{(i)}(t)dt}{A^*} \ , \tag{2}$$

where t is in seconds and A^* is the true gettered surface area.

3. RESULTS

Figure 2 exhibits the behavior of the partial pressures of masses 28 and 32, the major components of air, the leak gas. In this figure, the background pressures are shown at time 1. At time 2 the leak valve was opened with $Q_{\mathrm{leak}} = 1 \times 10^{-4}$ torr·L/s and power was applied to the chromium source. The rise in mass 28 is mostly due to outgassing from the source and the area of the vacuum wall close to the source, while the initial low value of mass 32 is due to wall pumping. Outgassing of other gas species also occurred, as shown by Fig. 3. As the temperature of the chromium source began to rise, large quantities of H_2 were evolved, which made the total pressure appear to be less than the

mass 28 partial pressure (Fig. 2) since the ion gauge factor for H_2 was 4 instead of 1.9 for air. Approximately 100 monolayers of chromium were deposited on the wall during a 30-min period. Power was removed from the source at time 3. Masses 2, 18, and 28 were all gettered, but the drop in pressure during the deposition of chromium is partially due to decreases in the outgassing rates of these gases. The partial pressure of mass 28 began to rise soon after the deposition ended and then rose to a value slightly higher than the equilibrium pressure. This behavior was due to the competition for sites by oxygen and then to the ability of this much more active gas to replace the nitrogen on the surface of the getter film [7]. The partial pressure of CO_2 increased by almost an order of magnitude when the air leak was started. This was due to the oxidation of carbon and CO by the available O_2 in the air leak. During the gettering of O_2 by the chromium film, less oxygen was available to form CO_2, so that the partial pressure of this species remained very low but rose again as the getter film began to saturate with O_2. This experiment was repeated with similar results.

Figure 4 shows the pumping speeds for masses 28 and 32 as functions of surface coverage. Curve A indicates that a break in the diffusion coefficient of O_2 occurs when the surface coverage reaches a value of 4×10^{16} particles per cm^2 with a roughness factor of unity, while curve C indicates that the surface is saturated by N_2 + CO with surface coverage of $\sim 8 \times 10^{15}$ particles per cm^2. However, the behavior of mass 28 is very complex for reasons given earlier and because it was a mixture of N_2 and CO. Curve D shows the results of an experiment in which N_2 was substituted for the air leak. In this case saturation occurred with surface coverage of $\sim 4 \times 10^{15}$ particles per cm^2. If we assume that only one monolayer (5×10^{14} particles per cm^2) of N_2 is absorbed on the getter surface, the roughness factor becomes 8. Curve B shows the getter pumping speed for oxygen as a function of the surface coverage for the true surface area, which is 8 times the projected area. This curve also shows that ~10 monolayers of O_2 are pumped by the film when the change in the diffusion coefficient occurs, which agrees with the results reported by Sakisaki [8]. A total of 9.31 torr·L of O_2 was injected during the experiment, and 6.4 torr·L was pumped by the getter, yielding an efficiency of 68.7%.

The enhanced plasma performance observed in ISX and TFTR was not entirely due to the high pumping speed for O_2 by the chromium film. Some of the gaseous impurities that evolve from the walls of tokamaks are not pumped very well by the chromium getter.

Many species that are pumped, for example nitrogen, do not diffuse into the bulk and are replaced by oxygen on the surface. Nevertheless, a reduction in the number of some of these particles in the vacuum has been observed. This effect is illustrated for masses 18, 28, and 44 in Figs. 5(a), (b), and (c), respectively, which show the results of rate-of-rise measurements. Curve A in each figure is from measurements made before the first chromium deposition and represents outgassing from the bare stainless steel surface. Curve B represents conditions after full saturation of the getter and exposure to ~3-torr pressure as a result of a vacuum accident, followed by exposure of the vacuum chamber to the atmosphere. The data labeled C in the figures were taken just prior to the onset of getter saturation by oxygen, and those labeled D represent data taken 4.5 h after saturation. Finally, E represents measurements taken 30 days later. These results clearly show decreases in the outgassing rates for masses 18, 28, and 44, even though these gas species are no longer being pumped by the getter, and thus illustrate the contribution toward the decrease of impurities in the vacuum resulting from surface coverage by the chromium film.

Figure 8 shows the results of the rate-of-rise measurements for masses 12 and 14 taken 4.5 h after saturation of the film by O_2. From the ratio of these rates we conclude that the majority of mass 28 was CO.

4. CONCLUSIONS

Water vapor, N_2/CO, and CO_2 were among the gases that were outgassed from the chromium source and the heated portions of the vacuum vessel walls during deposition of the chromium film. These species, along with the N_2 and O_2 from the leak gas (air), were also gettered as long as the deposition process continued. However, all these gases ceased to be pumped at any appreciable rate shortly after the deposition of chromium was discontinued. This was mainly because of the competition for sites by O_2. The particles of these species were replaced by O_2. Oxygen continued to be gettered by the film to a depth of about 10 monolayers when a break in the diffusion coefficient occurred and the pumping speed again became nearly constant but at a small fraction of the maximum (in this case 0.003%). The initial increase in the partial pressure of CO_2 was due to the oxidation of carbon and CO by the injected O_2, while the decrease in the pressure of this species throughout the period when oxygen was gettered was due to the lack of available O_2. As

the pumping speed for O_2 began to decrease, the partial pressure of CO_2 increased due to the increased availability of O_2 for these reactions. By means of an additional experiment in which N_2 replaced air as the leak gas, the surface roughness factor for the vacuum vessel wall was determined to be 8. The mechanism that produced a reduction in gas impurities other than O_2 was the coverage of the vacuum vessel walls by chromium, which reduced wall outgassing. This produced a long-lasting result that was still observed 30 days later.

REFERENCES

1. J. E. Simpkins, P. K. Mioduszewski, and L. W. Stratton, *J. Nucl. Mater.* **111,112** (1982) 827.
2. J. E. Simpkins, W. A. Gabbard, L. C. Emerson, and P. K. Mioduszewski, *J. Nucl. Mater.* **122,123** (1984) 1481.
3. P. K. Mioduszewski et al., *J. Nucl. Mater.* **128,129** (1984) 884.
4. H. F. Dylla et al., *J. Vac. Sci. Technol.* (in press).
5. W. R. Blanchard, *J. Vac. Sci. Technol.* (in press).
6. Varian Associates model 951–5106 variable leak valve.
7. J. E. Simpkins, L. C. Emerson, and P. K. Mioduszewski, *J. Vac. Sci. Technol.* **A1**(2) (1983) 1306.
8. Y. Sakisaki, H. Kato, and M. Onchi, Surf. Sci. **120** (1982) 150.

Fig. 1. Schematic of the experimental arrangement.

Fig. 2. Partial pressures of masses 28 and 32, the major components of the leak gas, as functions of time.

Fig. 3. Partial pressures of masses 2, 18, and 44 as functions of time.

Fig. 4. Film pumping speeds for mass 32 (A) and mass 28 (C), for pure N_2 (D), and for mass 32 (B) corrected for surface roughness.

Fig. 5. Rate of rise of masses (a) 18, (b) 28, and (c) 44 before gettering (A), after a vacuum accident that produced total saturation of the getter film (B), during saturation by O_2 (C), 4.5 h after saturation (D), and 30 days later (E).

Fig. 6. Rate of rise of masses 12 and 14 measured 4.5 h after saturation.

ORNL-DWG 86-2305 FED

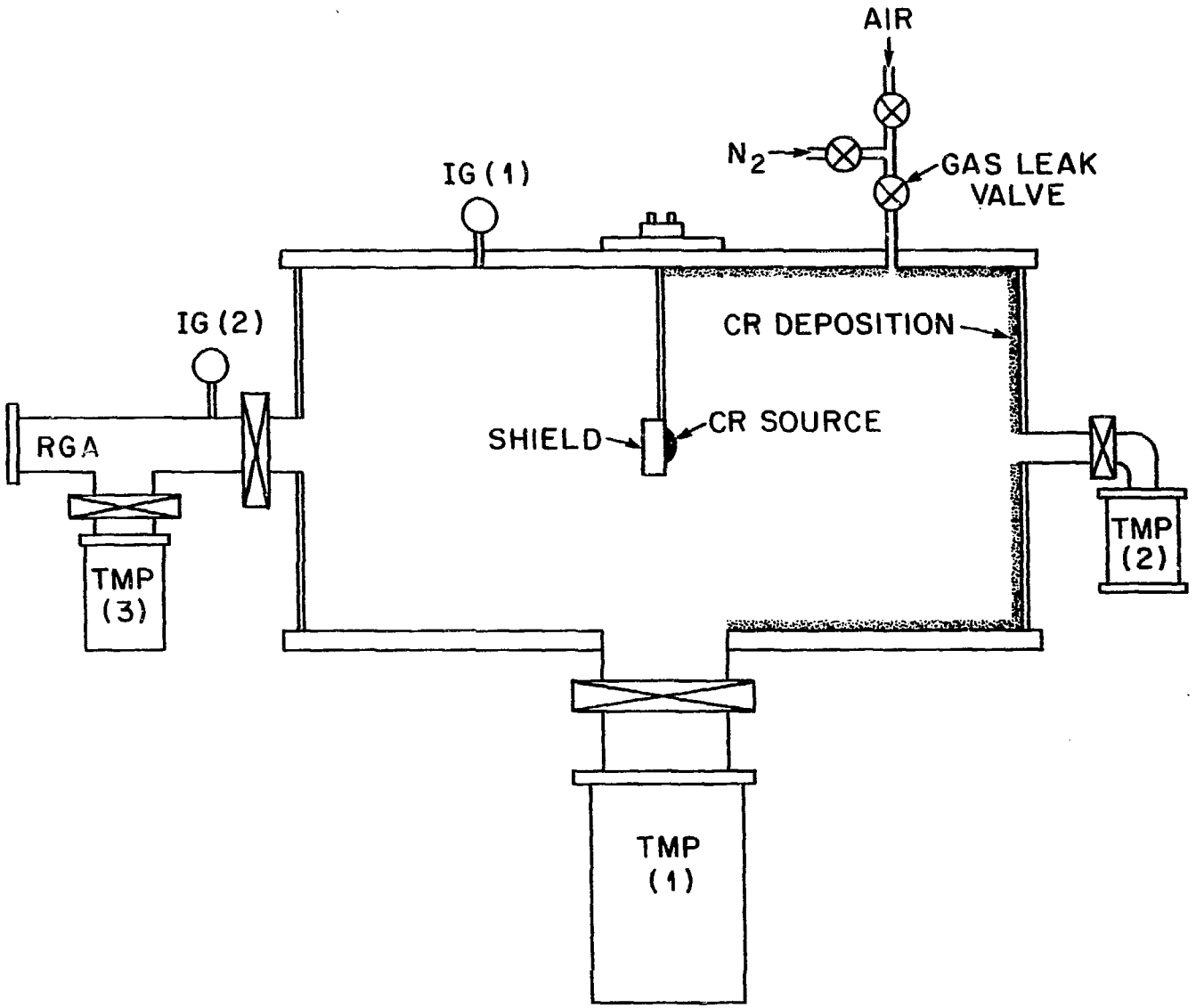

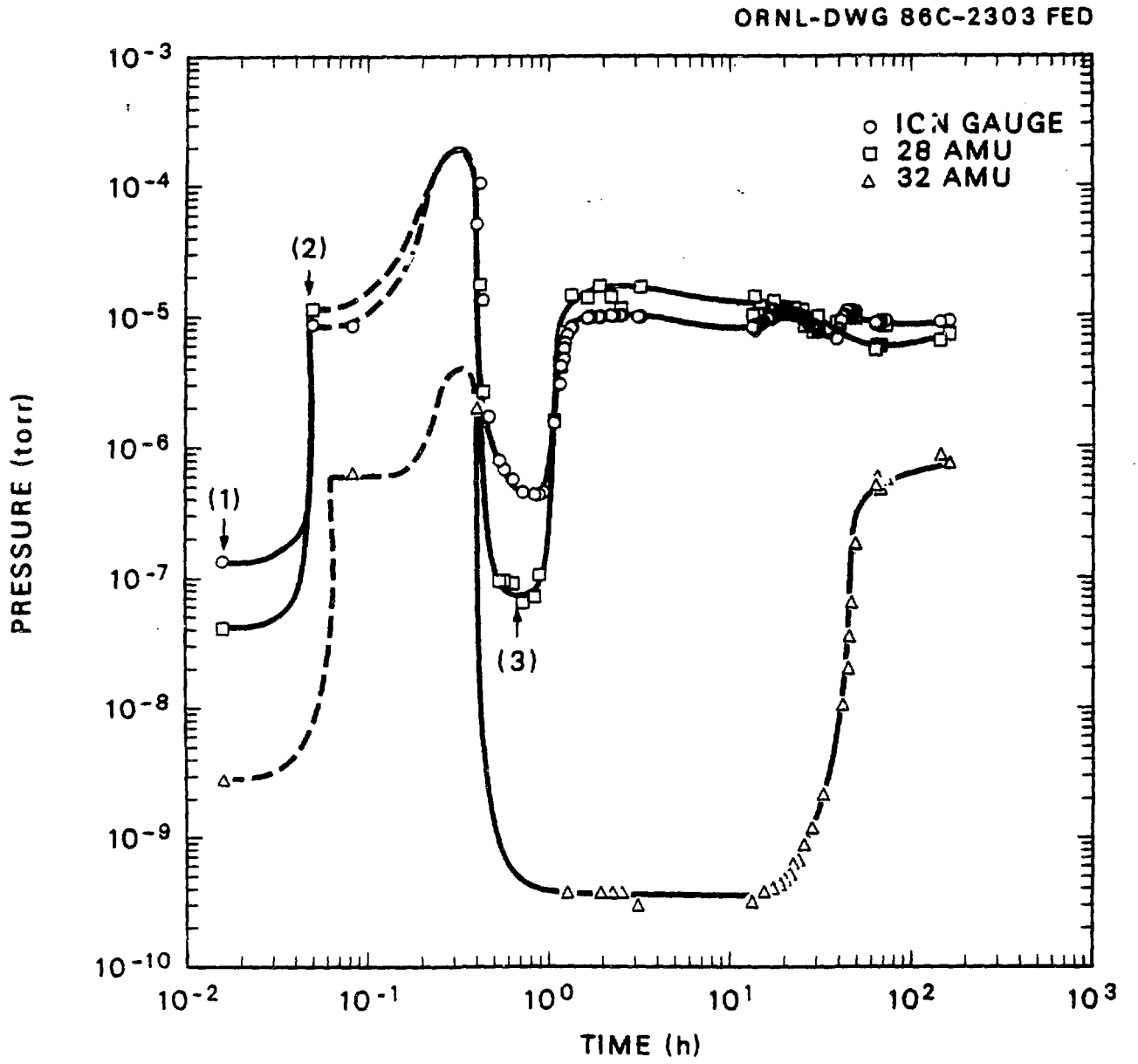
ORNL-DWG 86C-2303 FED
ION GAUGE
28 AMU
32 AMU
(1)
(2)
(3)
PRESSURE (torr)
TIME (h)
10^-3
10^-4
10^-5
10^-6
10^-7
10^-8
10^-9
10^-10
10^-2
10^-1
10^0
10^1
10^2
10^3

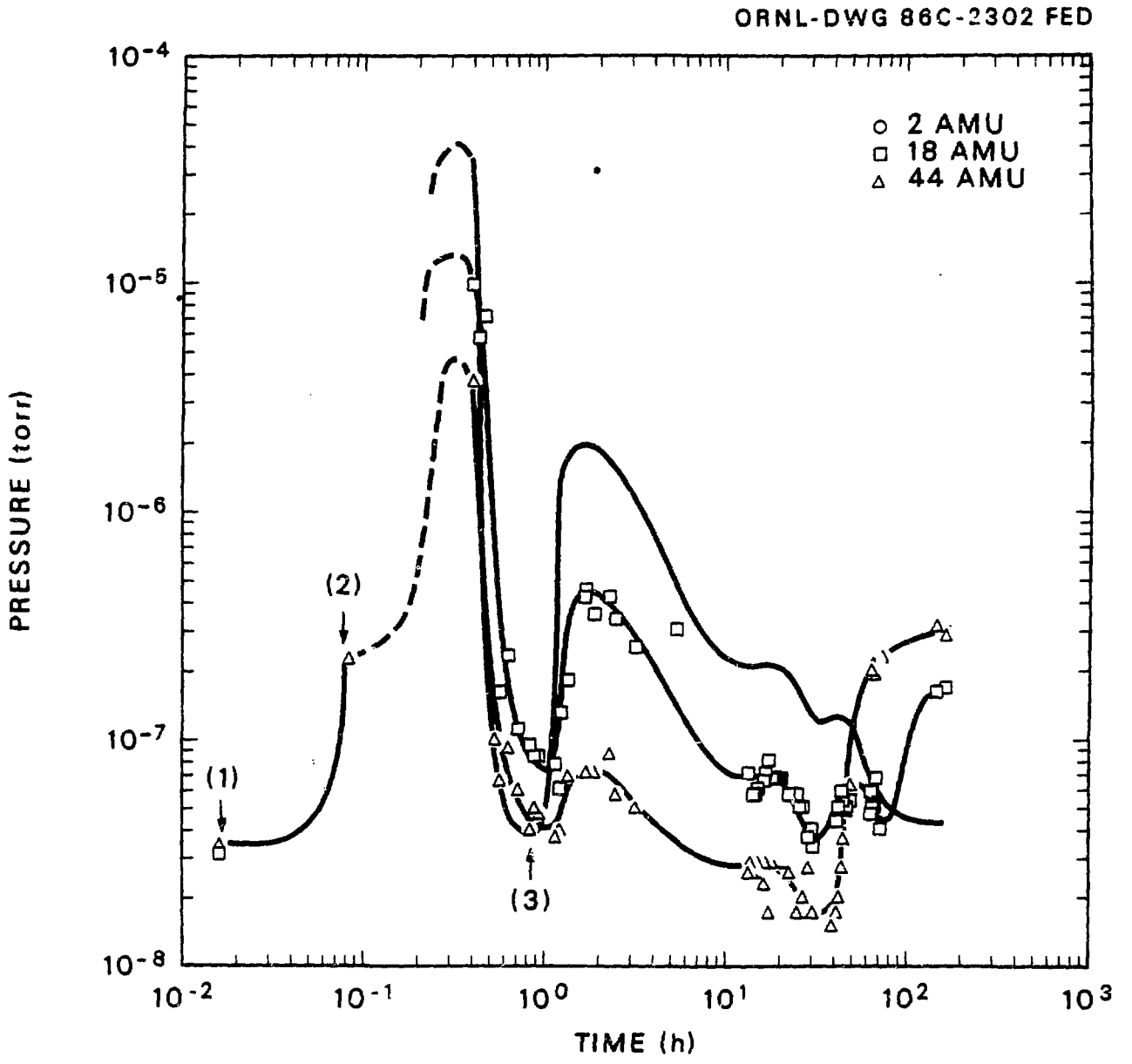
ORNL-DWG 86C-2302 FED
2 AMU
18 AMU
44 AMU
PRESSURE (torr)
TIME (h)
(1)
(2)
(3)

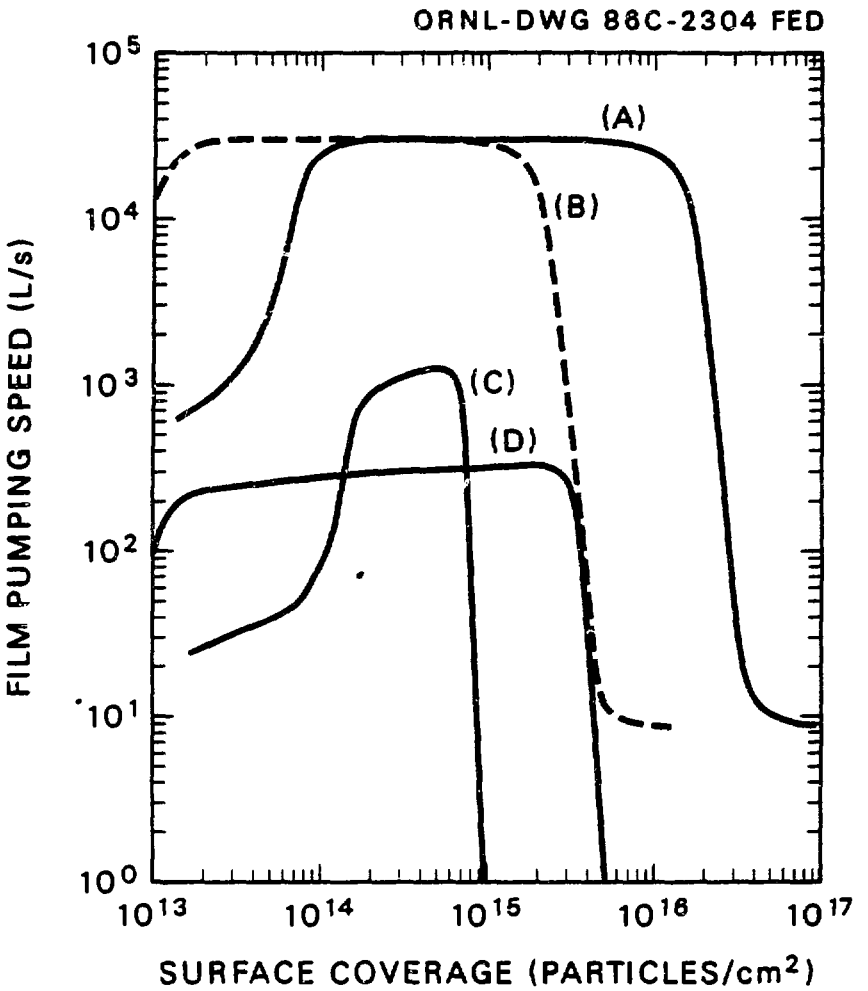
ORNL-DWG 86C-2304 FED
FILM PUMPING SPEED (L/s)
10^5
10^4
10^3
10^2
10^1
10^0
(A)
(B)
(C)
(D)
10^{13}
10^{14}
10^{15}
10^{16}
10^{17}
SURFACE COVERAGE (PARTICLES/cm^2)

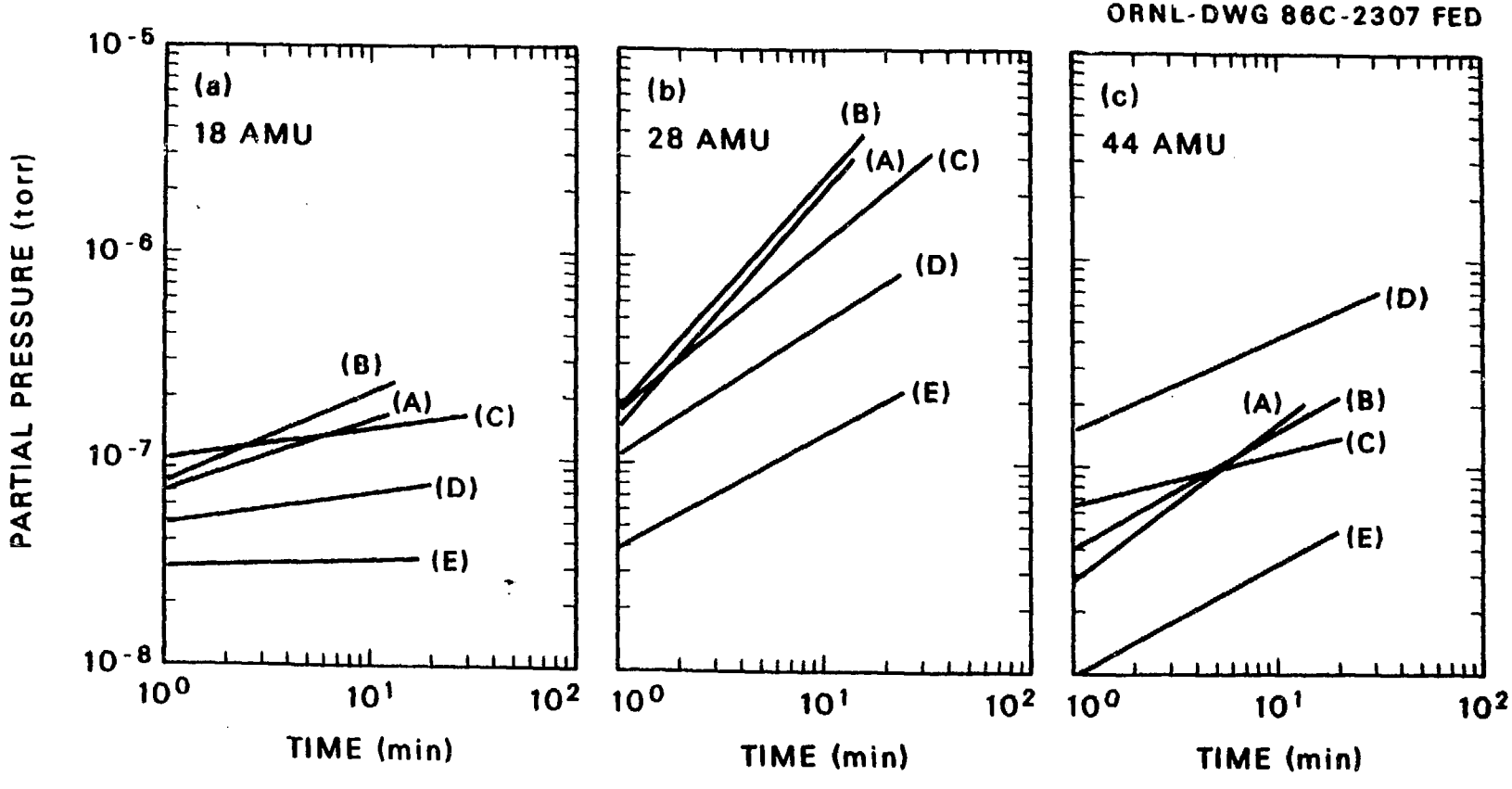
ORNL-DWG 86C-2307 FED
PARTIAL PRESSURE (torr)
10^{-5}
10^{-6}
10^{-7}
10^{-8}
(a)
18 AMU
(B)
(A)
(C)
(D)
(E)
10^0
10^1
10^2
TIME (min)
(b)
28 AMU
(B)
(A)
(C)
(D)
(E)
10^0
10^1
10^2
TIME (min)
(c)
44 AMU
(D)
(A)
(B)
(C)
(E)
10^0
10^1
10^2
TIME (min)

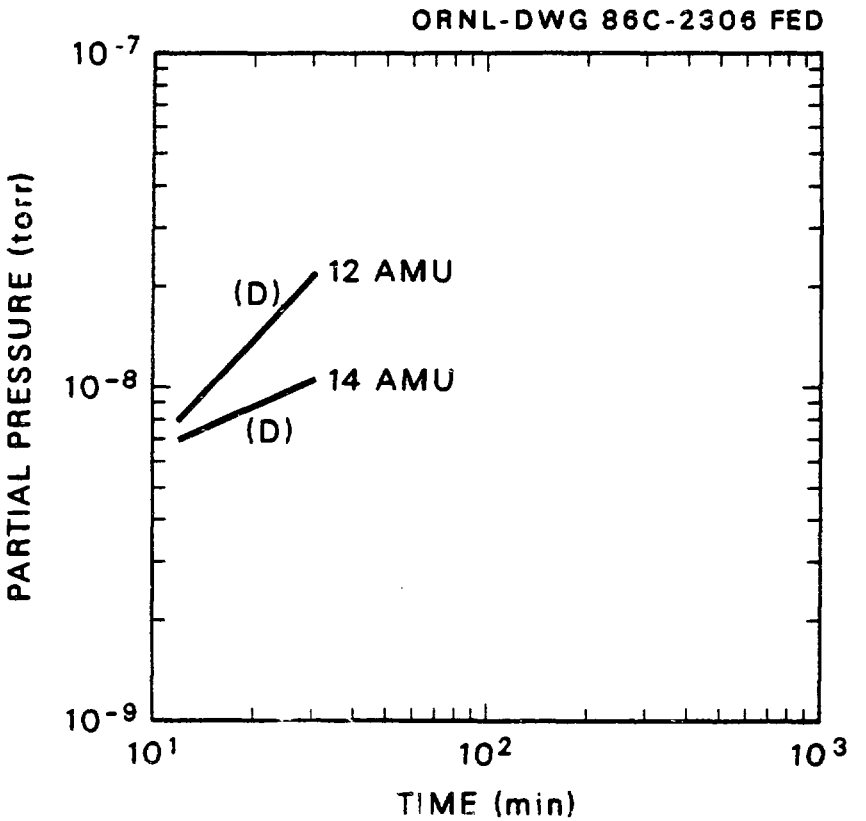
ORNL-DWG 86C-2306 FED
10^{-7}
10^{-8}
10^{-9}
PARTIAL PRESSURE (torr)
12 AMU
(D)
14 AMU
(D)
10^{1}
10^{2}
10^{3}
TIME (min)